This is the Pre-Published Version.

S. Lin, X. Huang (2020) *Quenching of Smoldering: Effect of Wall Cooling on Extinction*, **Proceedings of the Combustion Institute**, https://doi.org/10.1016/j.proci.2020.05.017

Quenching of Smoldering: Effect of Wall Cooling on Extinction

Shaorun Lin[1,2] and Xinyan Huang[1,*]

[1]*Research Centre for Fire Safety Engineering, Department of Building Services Engineering, The Hong Kong Polytechnic University, Hong Kong SAR*

[2]*The Hong Kong Polytechnic University Shenzhen Research Institute, Shenzhen, China*

*Corresponding author: xy.huang@polyu.edu.hk

Abstract

Smoldering fire is the slow, low-temperature, and flameless combustion phenomenon in porous fuels. Smoldering is different from flaming regarding the chemical and transport processes, despite sharing many similarities in ignition and fire spread. In this work, we explored the applicability of quenching and quenching diameter in smoldering. The smoldering of dry organic soil was initiated in the 25-cm long tubular reactor with different diameters from 4 cm to 15 cm. The thermal boundary and oxygen supply of the smoldering reactor were varied by using different wall materials and opening configurations, respectively. The quenching of smoldering was found as the diameter of the reactor decreased, the same as the quenching of the premixed flame. The minimum smoldering temperature (~250 ℃) and propagation rate (~0.5 cm/h or 0.1 mm/min) were found before quenching. The measured quenching diameter of smoldering was about 10 cm (much larger than the flame) and comparable to the thickness of reaction front (similar to the flame). The quenching diameter of smoldering increases as the wall cooling increases and the oxygen supply decreases. The influence of oxygen supply is unique to the smoldering quenching phenomenon as it affects the mode of smoldering propagation. This work helps understand the persistence and extinction limit of smoldering and the prevention and suppression strategies for smoldering fire.

Keywords: quenching diameter; fire behavior; smoldering propagation; oxygen supply; minimum temperature

1. Introduction

Quenching, in terms of combustion, refers to the flame extinction by cooling [1,2]. The quenching distance (or thickness/diameter) is a critical length below which flame can no longer propagate through [1,3]. Concepts of flame quenching and quenching distance are of practical significance in the design of flame arrestor [3], as well as, the fire protection system of many industrial equipment and processes. Fundamentally, the quenching of the premixed flame is attributed to the cooling from the reactor wall that decreases the flame temperature below the threshold of chain reaction [1]. The quenching behaviors and quenching distance of flame have been extensively studied, and key influence factors include the fuel type and concentration [4], thermal boundary [5,6], and flow conditions (laminar or turbulent) [7]. For a laminar premixed flame, quenching occurs on the scale of millimeter that is comparable to the flame thickness [1,2]. However, to the best of authors' knowledge, no study has systematically addressed the quenching dynamics of smoldering and quantified the corresponding quenching distance, thus, there is a big knowledge gap.

Smoldering is the slow, low-temperature, and flameless burning of porous fuels, and is the most persistent type of combustion [8,9]. Smoldering can be easily initiated by a weak heat source or even self-ignited, such as those in silos and storage units [10,11]. Once ignited, it is extremely difficult to extinguish [8,12], such as the smoldering firebrands [13] and peat soils [14,15] in wildland fire. In general, there are many similarities between

flaming and smoldering fire behaviors [8,15,16]. For solid fuels, pyrolysis is a necessary step for both smoldering and flaming ignition, and transition often occurs between flaming and smoldering [17–19]. For charring materials, fire-spread modes of both flaming and smoldering can be maintained, and both fire-spread rates vary with the fuel type, oxygen supply (or wind), and heat losses [8,15]. Therefore, it is reasonable to expect the quenching and quenching distance (or diameter) of smoldering like those of flame.

On the other hand, smoldering is also very different from the flaming in terms of combustion chemistry, transport processes, and time scales [8]. Fundamentally, the flame is dominated by the homogeneous oxidation of gaseous fuel, while smoldering is sustained by the heterogeneous oxidation on the surface of solid fuel [8,18]. The characteristic temperature (~500 °C), propagation rate (~1 cm/h), and heat of combustion (~10 MJ/kg) of smoldering are lower than those of flame [8,15,16,18–22]. The extinction of smoldering occurs with the increasing fuel moisture content [23], the decreasing pressure [24], and oxygen concentration [25,26] or by using suppression agents [12,27]. Rein [8,9] predicted the critical sample size of 15 cm for sustaining smoldering in the rectangular polyurethane foam, but it has not been verified by the experiment.

The purpose of this experimental study is to explore whether the classical concept of flame quenching and quenching diameter can be extended to smoldering. Considering the heat loss and oxygen supply are two key parameters that control the burning and propagation of smoldering [8], different conditions of wall cooling and oxygen supply were applied to the reactor to determine the quenching limit of smoldering. The quenching diameter was compared with the thickness of the smoldering front, and the minimum values of the smoldering temperature and propagation rate before quenching were quantified.

2. Experiment

2.1. Setup and controlling parameters

The dry organic peat soil, as a representative fuel that is prone to smolder, was chosen in the experiment (Fig. 1a). This type of moss peat soil has an organic content of above 95%, and was studied previously in [15,18,23]. The element analysis of peat sample shows 44.2, 6.1, 49.1, 0.5, 0.1% mass fractions for C, H, O, N and S, respectively. Before the test, the peat soil was first oven-dried at 90 °C for 48 h [15], and its bulk density and porosity were measured to be 150 ± 10 kg/m^3 and 0.90, respectively [18]. The shape of the peat soil particle was coarse, and its size was about 1 mm, leaving a large pore space between particles [22].

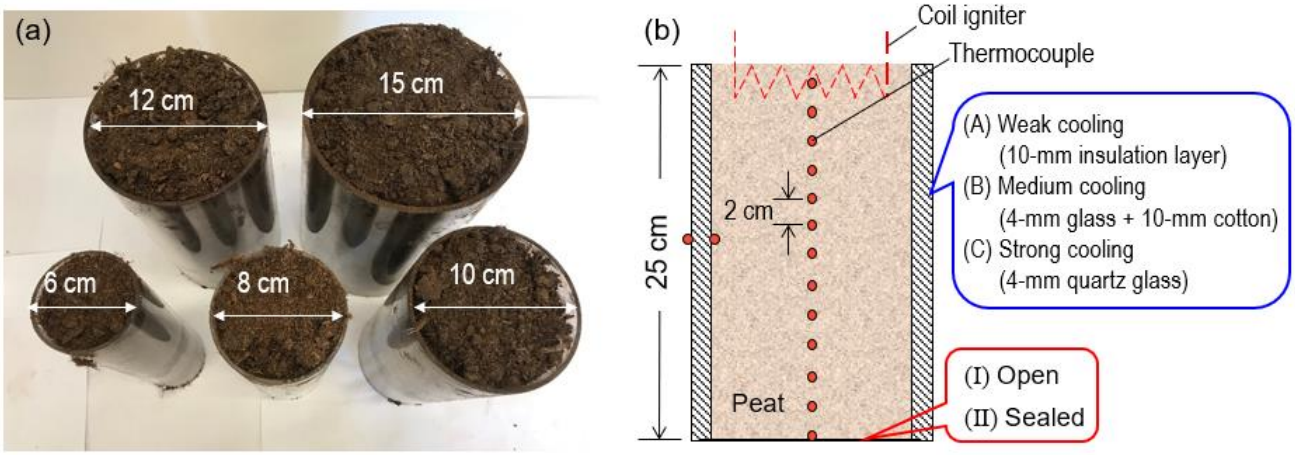

Fig. 1. (a) Photos of peat soil and tubular smoldering reactors with different diameters, (b) schematic diagrams for the smoldering reactor, and controlling parameters of wall cooling and oxygen supply.

The peat soil was filled into a group of 25-cm long tubular smoldering reactors with different diameters (D) from 4 cm to 15 cm, as shown in Fig. 1. Such tubular reactors were also widely used in other smoldering experiments [28,29]. Three reactor walls of different thermal resistances (R) were selected to vary wall cooling:

(A) *Weak cooling*: 10-mm ceramic insulation layer (0.1 W/m-K) with R_A (thermal resistance) = 0.1 m^2-K/W;

(B) *Medium cooling*: 4-mm quartz glass (1.0 W/m-K) covering by 10-mm cotton insulation layer (0.15 W/m-K) with R_B = 0.06 m^2-K/W, and

(C) *Strong cooling*: 4-mm quartz glass (1.0 W/m-K) with R_C = 0.004 m^2-K/W.

The smoldering reactor was vertically placed with the top surface open. To vary the oxygen supply to the reactor, the bottom surface was kept open with metal mesh to hold the fuel (i.e., a good oxygen supply) or sealed by the insulation board (0.05 W/m-K) (i.e., a poor oxygen supply), as illustrated in Fig. 1(b). The ambient temperature is 23 ± 2 ℃, and the relative humidity is about 50 ± 10 %.

2.2. Ignition method and test procedures

A coil heater was placed 1 cm below the fuel top free surface. The ignition protocol was fixed at 100 W for 0.5 h, the same as previous work [22,23], which was strong enough to initiate smoldering. Unlike the visible flame propagation, it was difficult to judge the success of smoldering propagation by visual observation [15,18]. Therefore, an array of 13 K-type thermocouples with the 100-μm bead was inserted into the sample along the axis. These thermocouples were placed from 1 cm to 25 cm below the top free surface with the 2-cm interval to monitor the temperature and the location of the smoldering front [22]. Temperatures of inner and outer wall surfaces were also measured by two thermocouples (~13 cm below the free surface), as shown in Fig. 1(b).

Quenching test was started with the largest reactor (D =15 cm). If smoldering successfully propagated to the bottom, the reactor diameter was then decreased gradually until the smoldering front could no longer propagate, i.e., the smoldering quenching, so that the quenching diameter (D^*) could be determined. Afterward, conditions of wall cooling and oxygen supply were changed to explore the variation of quenching diameter. For each scenario, tests were repeated at least twice, and good experimental repeatability was found.

3. Results and discussions

3.1. Smoldering quenching phenomena

Figure 2(a) shows the thermocouple measurements of a successful smoldering propagation in the 15-cm wide reactor with the bottom sealed under the weak cooling. Once ignited, the smoldering front gradually propagated downward, and the temperature decreased from 500 ℃ to 350 ℃ with increasing depth. After 48 h, most of the peat soils burnt into ash with the mass loss above 90% of the original mass. Figure 2(b) shows an example of smoldering quenching (or failed propagation) through a 6-cm wide reactor. During ignition, the sample temperature could reach about 500 ℃, but after ignition, it gradually decreased to ambient temperature within 5 h. For all quenched cases, the mass loss of peat soil was below 20% of the original mass.

To better compare different cooling conditions of the reactor wall, the approximate and simplified one-dimensional cooling flux through the wall ($\dot{q}''_w$) in the slow and quasi-steady-state smoldering propagation may be expressed as:

$$\dot{q}''_w = \frac{T_{wi} - T_{wo}}{R_w} = h(T_{wo} - T_\infty) + \varepsilon\sigma(T_{wo}^4 - T_\infty^4) \approx k_F \frac{T_{sm} - T_{wi}}{D/2} \quad (1)$$

where T_{sm} is the characteristic temperature of smoldering, T_{wi} and T_{wo} are the inner and outer wall

temperatures, T_∞ is the ambient temperature, h is convective coefficient, ε is the emissivity, σ is the Stefan-Boltzmann constant, and k_F is the thermal conductivity of fuel. The thermal resistance of the reactor wall is $R_w = \sum \delta_i/k_i$, where δ_i and k_i are the thickness and thermal conductivity of i^{th} wall layer, respectively. Based on temperature measurements in the experiment, cooling fluxes for three walls were $\dot{q}''_{wA}$ = 1.0 ± 0.1 kW/m^2 (weak cooling), $\dot{q}''_{wB}$ = 1.6 ± 0.3 kW/m^2 (medium cooling), and $\dot{q}''_{wC}$ = 2.4 ± 0.6 kW/m^2 (strong cooling).

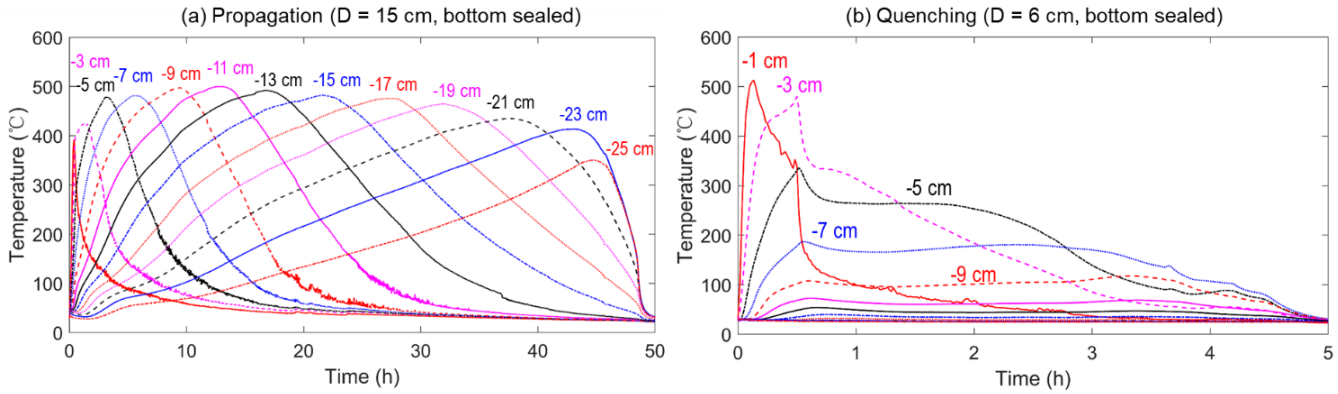

Fig. 2. Thermocouples data of (a) successful smoldering propagation in the 15-cm wide reactor, and (b) smoldering quenching in the 6-cm wide reactor with the bottom sealed under a weak wall cooling (1 kW/m^2). The negative sign means that the thermocouple is below the reactor's top free surface.

3.2. Quenching diameter of smoldering

The experimental outcomes of smoldering propagation (●) and quenching (×) are summarized in Fig. 3. The quenching of smoldering occurs as the diameter of reactor decreases, and the quenching diameter increases as the cooling flux increases. Therefore, both smoldering quenching behaviors are essentially the same as the quenching of the premixed flame [4–6]. Specifically, if the oxygen supply is good by opening the bottom of reactor (Fig. 3a), as the wall cooling flux increases from 1 kW/m^2 to 2.4 kW/m^2, the quenching diameter increases from 5 ± 1 cm to 11 ± 1 cm. Note that the smoldering quenching diameter has a length scale of several centimeters, which is 1~2 orders of magnitude larger than the flaming quenching distance (~1 mm) [1–5].

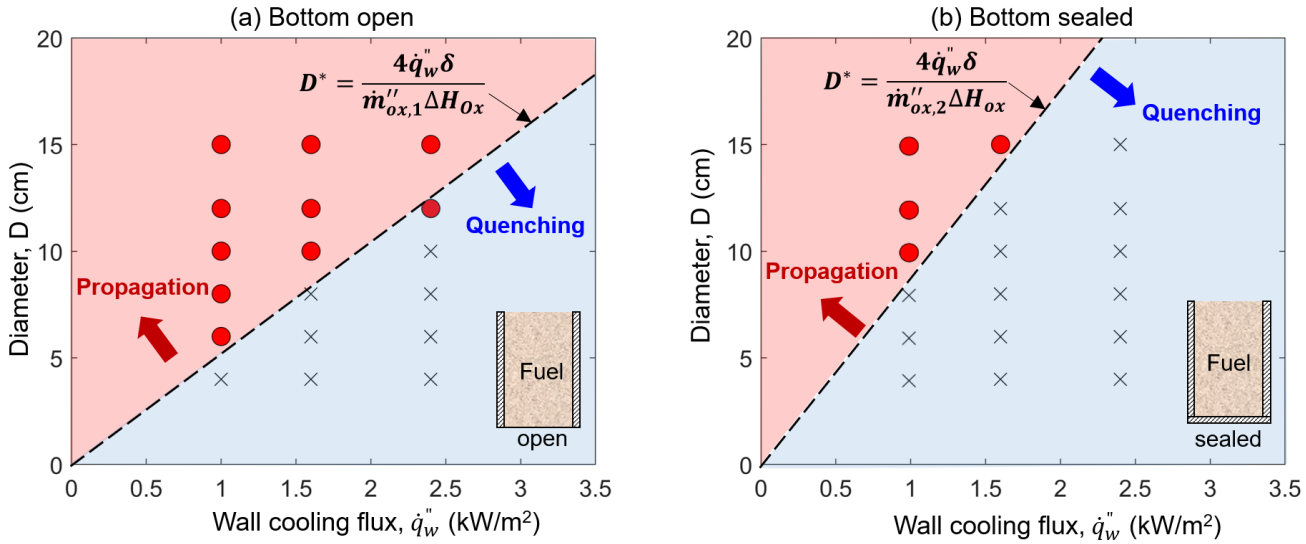

Fig. 3. Experimental outcomes of (a) bottom open with a good oxygen supply, and (b) bottom sealed with a poor oxygen supply, where smoldering propagation uses ● and quenching uses ×.

To further explain the influence of wall cooling on the smoldering quenching diameter (D^*), a simplified energy conservation equation is applied to a propagating smoldering front with the thickness of δ, as illustrated in Fig. 4(a). At the quenching diameter (D^*), the heat loss from the cold wall ($\dot{Q}_w$) is equal to the heat generation from the smoldering zone ($\dot{Q}_{sm} = \dot{Q}_{ox}$) due to oxidation as

$$\dot{Q}_w = \dot{Q}_{sm} = \dot{Q}_{ox} \tag{2}$$

$$\dot{q}_w''(\pi D^* \delta) = \dot{m}_F'' \left(\frac{\pi}{4} D^{*2}\right) \Delta H_F = \dot{m}_{ox}'' \left(\frac{\pi}{4} D^{*2}\right) \Delta H_{ox} \tag{3}$$

$$D^* = \frac{4\dot{q}_w'' \delta}{\dot{m}_F'' \Delta H_F} = \frac{4\dot{q}_w'' \delta}{\dot{m}_{ox}'' \Delta H_{ox}} \tag{4}$$

where $\dot{m}_F''$ is the smoldering burning flux of fuel, ΔH_F is the heat of smoldering combustion of fuel which is sensitive to the burning conditions, $\dot{m}_{ox}''$ is the mass flux of oxygen (i.e., the rate of oxygen supply), and ΔH_{ox} is the heat of oxidation. A similar expression was previously derived for the rectangular fuel sample in [9]. Equation (4) reveals that the smoldering quenching diameter is proportional to the wall cooling flux, which explains the trend of experimental data in Fig. 3.

If the oxygen supply is reduced by sealing the bottom of the reactor (Fig. 3b), the quenching diameter also increases with the wall cooling flux, following the same trend of the bottom-open case in Fig. 3(a). On the other hand, under the same cooling flux, quenching becomes easier, and the quenching diameter increases, because of the reduced oxygen supply from the bottom. Specifically, at the cooling flux of 1 kW/m^2, the quenching diameter (D^*) increases from 5 ± 1 cm with the bottom open to 9 ± 1 cm with the bottom sealed. Such a trend can also be explained by Eq. (4), where the quenching diameter is inversely proportional to the rate of oxygen supply ($\dot{m}_{ox}''$).

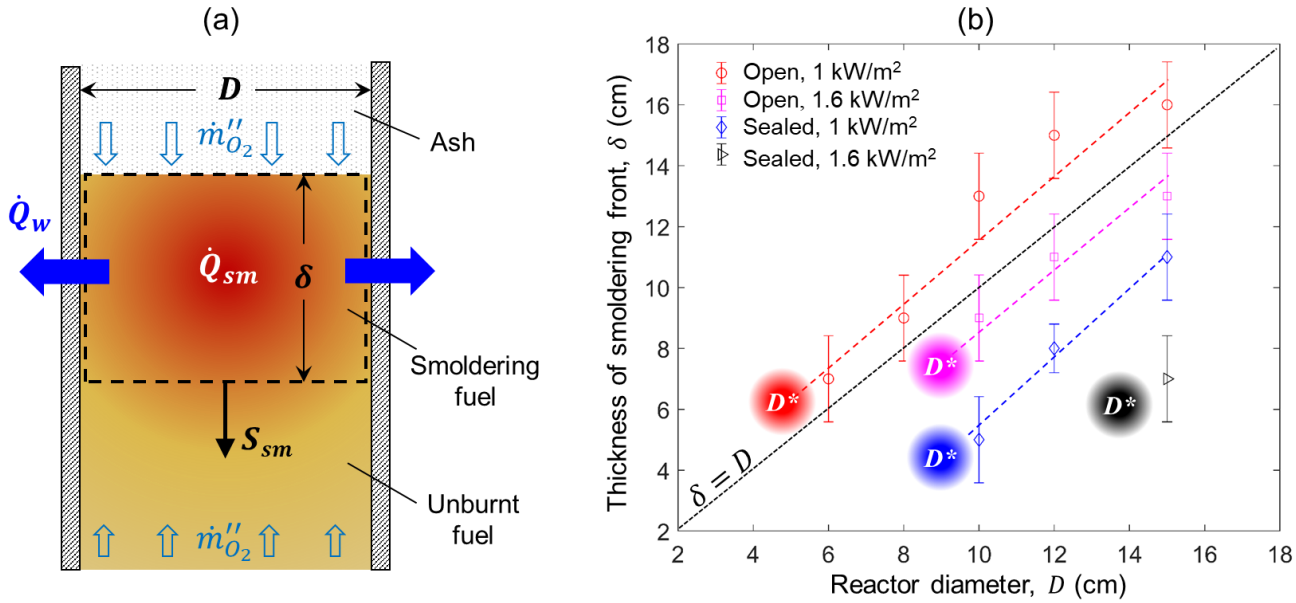

Fig. 4. (a) Schematics for smoldering quenching, and (b) thickness of smoldering front (δ) *vs*. reactor diameter (D), where the shadowed point indicates the quenching diameter (D*) and minimum thickness (δ*).

3.3. Smoldering front thickness

By defining a minimum smoldering temperature of 250 ℃, the average thickness of smoldering front (δ) in successfully propagated cases can be estimated based on the thermocouple data (e.g. Fig. 2a). Figure 4(b) summarizes the thickness of the smoldering front, which increases with the reactor diameter as well as the oxygen supply. For example, with the bottom open and the weak cooling flux of 1 kW/m^2, the thickness of the smoldering front increases from 7 cm to 16 cm, as the reactor diameter increases from 6 cm to 15 cm.

Table 1. Measured quenching diameter (D^*) and minimum smoldering front thickness (δ^*).

Wall cooling	**Weak**		**Medium**		**Strong**	
Oxygen supply	**Open**	**Sealed**	**Open**	**Sealed**	**Open**	**Sealed**
$\dot{q}''_w$	1.0 ± 0.1		1.6 ± 0.3		2.4 ± 0.6	
D^* (cm)	5 ± 1	9 ± 1	9 ± 1	13.5 ± 1.5	11 ± 1	>15
δ^* (cm)	6 ± 1	4 ± 1	7 ± 1	6 ± 1	7 ± 1	-
D^*/δ^*	0.8 ± 0.1	2.3 ± 0.6	1.3 ± 0.1	2.3 ± 0.5	1.6 ± 0.3	-

Moreover, the minimum thickness of the smoldering front (δ^*) can be estimated by a linear extrapolation towards the quenching diameter, as indicated by the shadowed points in Fig. 4(b). As summarized in Table 1, the value of δ^* ranges from 4 to 7 cm, which is insensitive to the wall cooling, but slightly decreases with the decreasing oxygen supply. The comparison further shows that the minimum smoldering front thickness and the quenching distance are comparable (i.e., $D^* \sim \delta^*$). Such behavior is similar to the premixed flame whose quenching distance (or diameter) is comparable to flame thickness [1–5].

To further explain the relationship between the smoldering thickness and quenching diameter, the analogy could be made between the burning of premixed flame and smoldering propagation [9,15]. Considering a 1-step global smoldering reaction

$$\text{Fuel} + v\text{O}_2 \rightarrow (1+v)\ \text{Products} \tag{5}$$

Then, the smoldering burning flux of fuel can be described as

$$\dot{m}''_{ox}/v = \dot{m}''_F \approx \rho_F S_{sm} \tag{6}$$

where v = 1 ~ 2 is the oxygen stoichiometric coefficient [9,18], ρ_F is the fuel density, S_{sm} is the smoldering burning speed, and the burnout of fuel is assumed after smoldering propagation. By balancing the advection and diffusion terms in the energy equation like the laminar premixed flame [2], the smoldering burning speed (S_{sm}) could be approximated as

$$S_{sm} \approx \frac{2\alpha_F}{\delta} \tag{7}$$

where $\alpha_F = k_F/(\rho_F c_p)$ is the thermal diffusivity. The heat of smoldering can be estimated as

$$\Delta H_F \approx (1+v)c_p(T_{sm} - T_o) \tag{8}$$

where T_o is the initial temperature and c_p is the specific heat. By substituting Eqs. (1,6-8) into Eq. (4), the quenching diameter becomes

$$D^* \approx \frac{4k_F \dfrac{T_{sm}-T_{wi}}{D^*/2}\delta^*}{\rho_F \dfrac{2\alpha_F}{\delta^*}(1+v)c_p(T_{sm}-T_o)} = C\cdot\delta^* \tag{9}$$

where

$$C = 2\sqrt{\frac{1}{1+v}\left(\frac{T_{sm}-T_{wi}}{T_{sm}-T_o}\right)} \tag{10}$$

which explains why the smoldering quenching diameter is comparable to the thickness of the smoldering front in Fig. 4(b). As the wall cooling increases, the wall temperature (T_{wi}) decreases so that the ratio of D^*/δ^* increases. By sealing the reactor bottom, the smoldering temperature (T_{sm}) increases due to the change of smoldering-propagation mode (see more discussions in Section 3.5), so that the ratio of D^*/δ^* also increases. Both trends of D^*/δ^* are consistent with experimental measurements in Table. 1

3.4. Smoldering temperature and propagation rate

Figure 5 shows the effect of reactor diameter, wall cooling, and oxygen supply on the (peak) smoldering temperature (T_{sm}) and the (downward) propagation rate (S_{sm}). For this dry peat soil, the smoldering temperature is no more than 500 ℃, which is similar to the literature data [15,23], and as expected, it is much lower than the minimum temperature of flame (~1300 K) [2]. The propagation of smoldering is in a creeping manner (about 1 ~ 6 cm/h), which is at least two orders of magnitude slower than the flame-spread rate over solid fuel [3] or the burning velocity of premixed flame [2]. As the wall cooling increases, both the smoldering temperature and propagation rate decrease. For increasing the oxygen supply by opening the bottom, the smoldering propagation rate, as expected, increases significantly, but the smoldering temperature decreases, because of the change in mode of smoldering propagation (discussed in Section 3.5).

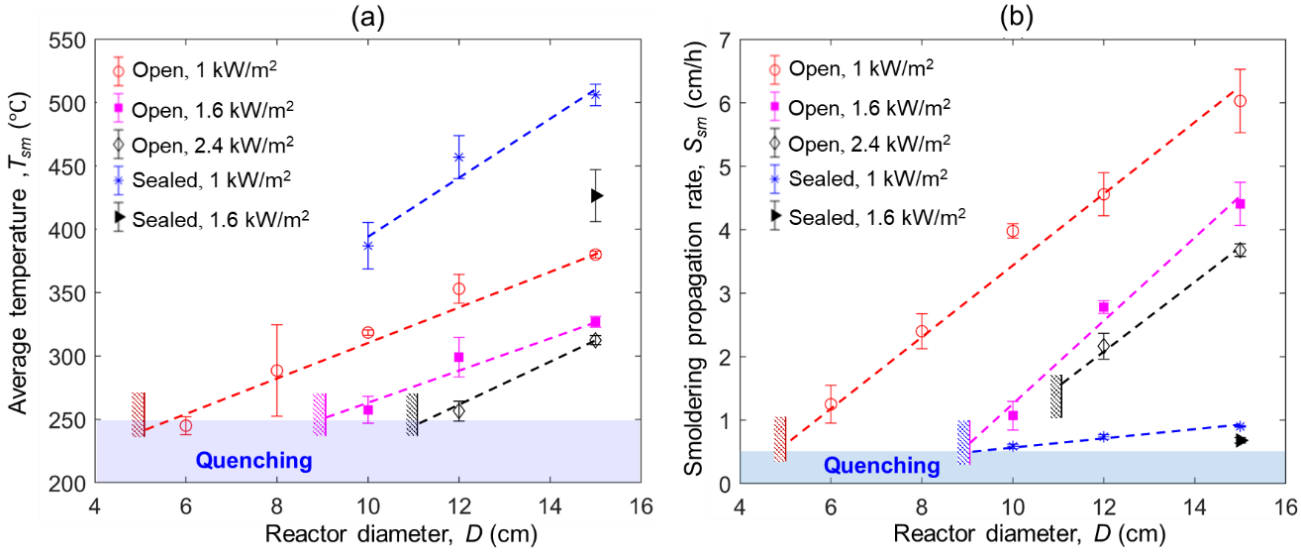

Fig. 5. (a) Mean smoldering temperature (T_{sm}), and (b) downward smoldering propagation rate (S_{sm}) as a function of reactor diameter (D), wall cooling flux, and oxygen supply.

Moreover, as the reactor diameter decreases, both the smoldering temperature and propagation rate continuously decrease. Eventually, at the quenching limit, the *minimum temperature to maintain smoldering* is

found to be about 250 °C, which is close to the threshold temperature for char oxidation found in the thermogravimetric analysis of this fuel [18]. Also, the *minimum smoldering propagation rate* before quenching is found to be about 0.5 cm/h or 0.1 mm/min.

3.5. Influence of oxygen supply

Figure 6 compares the temperature profile of successful smoldering propagation with (a) bottom sealed and (b) bottom open, where the reactor diameter is 12 cm and the weak cooling flux of 1 kW/m^2 is applied. For the bottom-sealed reactor in Figs. 2(a) and 6(a), after ignition, the smoldering front gradually propagates downward to the bottom and the top free surface regresses [22], as illustrated in Fig. 7(a). As the oxygen diffuses from the top free surface, it is forward smoldering propagation where the reaction front moves due to the burnout of fuel [15,22], similar to the motion of candle flame or the burning of premixed flame. After burnout, a sandwich residue structure is observed (Stage III in Fig. 7a) where the top and bottom thin layers of char is not burnt due to the heat loss to the environment [22].

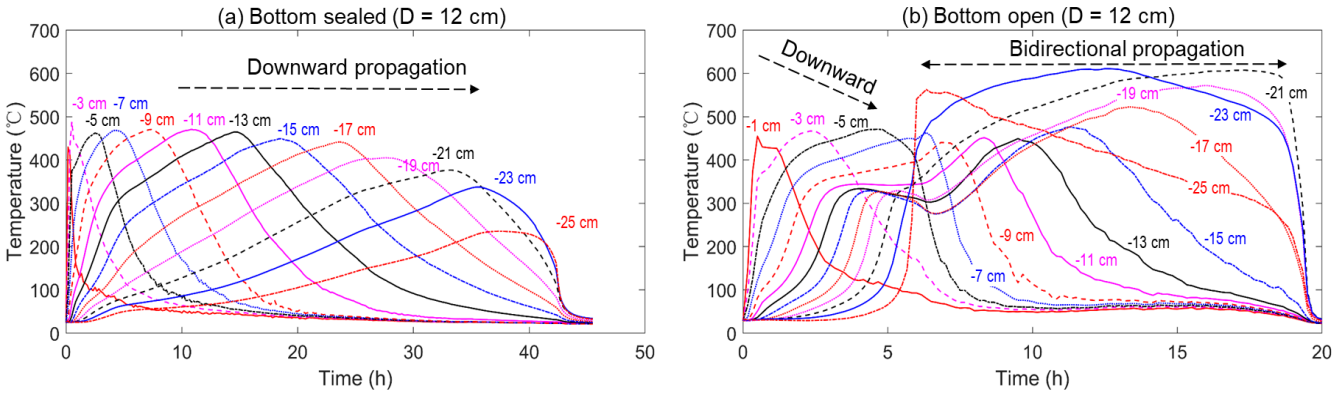

Fig. 6. Thermocouple data of smoldering propagation in the 12-cm wide reactor under the cooling flux of 1 kW/m^2, (a) bottom sealed with the downward propagation, and (b) bottom open with the downward-to-bidirectional propagation. The negative sign means thermocouple is below the reactor's top free surface.

With the reactor bottom open, there is an extra oxygen supply from the bottom, which could be dominant, due to the chimney effect, and much larger than the oxygen diffusion from the top [19]. In Fig. 6(b), the smoldering propagation has two stages, (1) 1st-stage downward propagation and (b) 2nd-stage bidirectional propagation, as illustrated Fig.7(b). Compared with bottom-sealed case in Fig. 6(a), the 1st downward propagation is faster, while the temperature is lower (see more comparisons in Fig. 5). Under the upward airflow, such a downward (opposed) propagation is fundamentally a continuous ignition process, that is, the newly ignited smoldering front moving towards the airflow [15]. Thus, it is different from the downward (forward) propagation in Figs. 6(a) and 7(a). Note that as small amount of oxygen still diffuses from the top surface, a slow burning process remains below the ash layer (see Stage II).

After the smoldering front reaches the bottom (about 6 h in Fig. 6b), both smoldering fronts on the top and bottom start to propagate towards the center, that is, a bidirectional forward propagation or burning (see Stage III and IV in Fig. 7b). Because of large oxygen supply and good insulation by ash layers, the 2nd-stage bidirectional has a higher temperature of about 600 °C, and the overall burnout time is about 20 h, much shorter than 45 h in the single-stage downward smoldering propagation in Fig. 6(a). Note that in experiment, as long as the 1-step propagation was successful, the second bidirectional propagation would not be quenched.

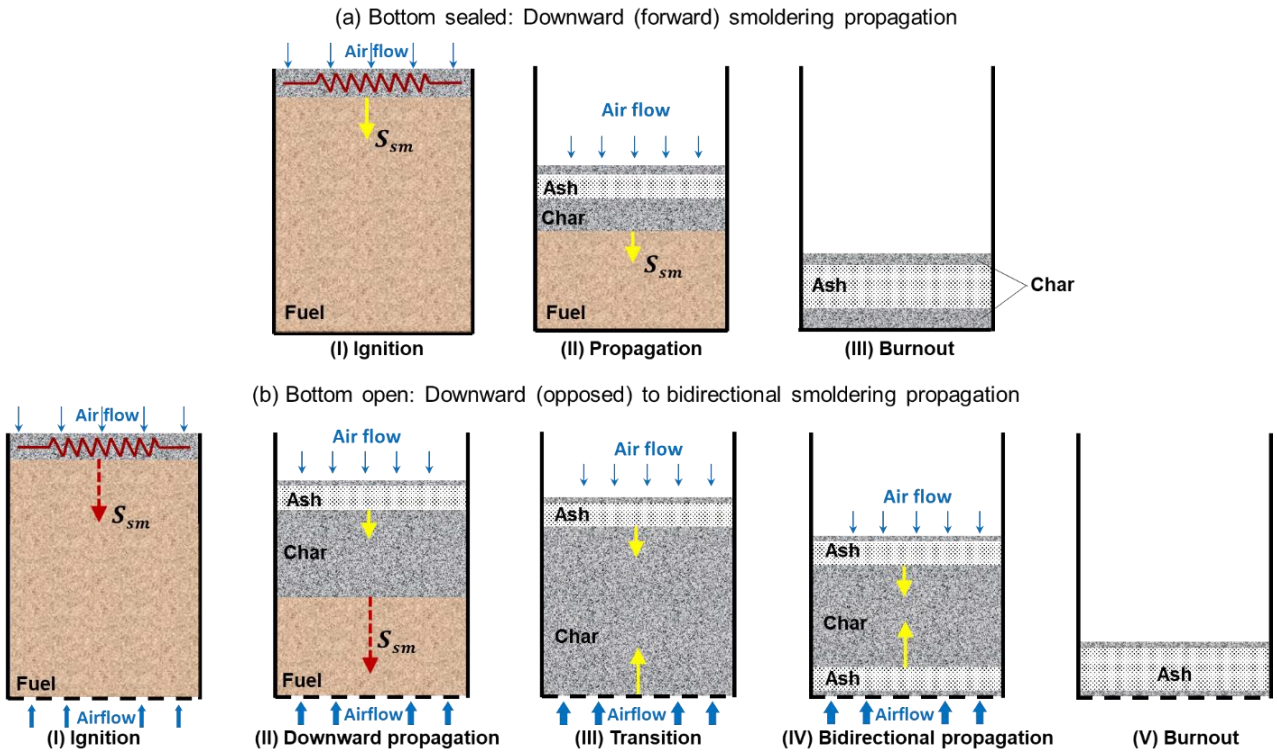

Fig. 7. Schematic diagrams of (a) single-stage downward (forward) smoldering propagation, and (b) 2-stage smoldering from downward (opposed) propagation to bidirectional propagation.

4. Conclusions

In this work, quenching of smoldering was observed as the reactor diameter decreased, which is the same as the quenching of flame. The smoldering quenching diameter was quantified for the first time, which is on the order of centimeter and much larger than the flame. Like the flame, the smoldering quenching diameter is also comparable to the thickness of the reaction front, and it increases as the wall cooling increases and the oxygen supply decreases, which are explained analytically. The minimum smoldering temperature (~250°C) and propagation rate (~0.5 cm/h or 0.1 mm/min) was found at the quenching limit.

The oxygen supply plays a unique role in smoldering propagation and quenching. By opening both ends of the reactor, the single-stage downward (forward) propagation transitions to the 2-stage downward-to-bidirectional propagation. Future experiments will be conducted to determine the smoldering quenching distance for different fuels and under controlled oxygen flux, and numerical simulations are needed to reveal the underlying physical process and heterogeneous chemistry behind the minimum smoldering temperature and propagation rate.

Acknowledgments

This study received financial support from the National Natural Science Foundation of China (NSFC grant No. 51876183), ZJU SKLCEU Open Fund (2018012), Sichuan Science and Technology Program (2019YFSY0040), and HK PolyU (1-BE04). The authors thank Prof. Cangsu Xu (Zhejiang University) for valuable discussion.

References

[1] Williams FA. Combustion Theory. 2nd ed. CRC Press; 1985.

[2] R.Turns S. An Introduction to Combustion: Concepts and Application. 3rd ed. India: McGraw-Hill

Education (India) Private Limited; 2012.

[3] Quintiere JG. Fundamentals of fire phenomena. John Wiley; 2006. doi:10.1002/0470091150.

[4] Bai B, Chen Z, Zhang H, Chen S. Flame propagation in a tube with wall quenching of radicals. Combustion and Flame 2013;160:2810–9. doi:10.1016/j.combustflame.2013.07.008.

[5] Kim N Il, Maruta K. A numerical study on propagation of premixed flames in small tubes. Combustion and Flame 2006;146:283–301. doi:10.1016/j.combustflame.2006.03.004.

[6] Veeraragavan A. On flame propagation in narrow channels with enhanced wall thermal conduction. Energy 2015;93:631–40. doi:10.1016/j.energy.2015.09.085.

[7] Haq MZ, Sheppard CGW, Woolley R, Greenhalgh DA, Lockett RD. Wrinkling and curvature of laminar and turbulent premixed flames. Combustion and Flame 2002;131:1–15. doi:10.1016/S0010-2180(02)00383-8.

[8] Rein G. Smoldering Combustion. SFPE Handbook of Fire Protection Engineering 2014;2014:581–603. doi:10.1007/978-1-4939-2565-0_19.

[9] Rein G. Smouldering Combustion Phenomena in Science and Technology. International Review of Chemical Engineering 2009;1:3–18.

[10] Babrauskas V. Ignition Handbook. Issaquah, WA: Fire Science Publishers/Society of Fire Protection Engineers; 2003. doi:10.1023/B:FIRE.0000026981.83829.a5.

[11] Huang X, Gao J. A review of near-limit opposed fire spread. Fire Safety Journal 2020:103141. doi:10.1016/j.firesaf.2020.103141.

[12] Lin S, Cheung YK, Xiao Y, Huang X. Can rain suppress smoldering peat fire? Science of the Total Environment 2020;726:138468. doi:10.1016/j.scitotenv.2020.138468.

[13] Manzello SL, Suzuki S, Gollner MJ, Fernandez-Pello AC. Role of firebrand combustion in large outdoor fire spread. Progress in Energy and Combustion Science 2020;76:100801. doi:10.1016/j.pecs.2019.100801.

[14] Rein G. Smouldering Fires and Natural Fuels. In: Claire M. Belcher, editor. Fire Phenomena in the Earth System, New York: John Wiley & Sons, Ltd.; 2013, p. 15–34. doi:10.1002/9781118529539.ch2.

[15] Huang X, Rein G. Upward-and-downward spread of smoldering peat fire. Proceedings of the Combustion Institute 2019;37:4025–33. doi:10.1016/j.proci.2018.05.125.

[16] Ohlemiller T, Lucca D. An experimental comparison of forward and reverse smolder propagation in permeable fuel beds. Combustion and Flame 1983;54:131–47. doi:10.1016/0010-2180(83)90027-5.

[17] Xie Q, Zhang Z, Lin S, Huang X, Polytechnic HK, Kong H, et al. Smoldering Fire of High-Density Cotton. Fire Technology 2020. doi:10.1007/s10694-020-00975-1.

[18] Lin S, Sun P, Huang X. Can peat soil support a flaming wildfire? International Journal of Wildland Fire 2019;28:601–13. doi:10.1071/WF19018.

[19] Santoso MA, Christensen EG, Yang J, Rein G. Review of the Transition From Smouldering to Flaming Combustion in Wildfires. Frontiers in Mechanical Engineering 2019;5. doi:10.3389/fmech.2019.00049.

[20] Anderson MK, Sleight RT, Torero JL. Downward smolder of polyurethane foam: Ignition signatures. Fire Safety Journal 2000;35:131–47. doi:10.1016/S0379-7112(00)00016-3.

[21] Torero JL, Fernandez-Pello a. C, Kitano M. Opposed Forced Flow Smoldering of Polyurethane Foam. Combustion Science and Technology 1993;91:95–117. doi:10.1080/00102209308907635.

[22] Huang X, Rein G. Downward Spread of Smoldering Peat Fire: the Role of Moisture, Density and Oxygen Supply. International Journal of Wildland Fire 2017;26:907–18. doi:10.1071/WF16198.

[23] Huang X, Restuccia F, Gramola M, Rein G. Experimental study of the formation and collapse of an overhang in the lateral spread of smouldering peat fires. Combustion and Flame 2016;168:393–402. doi:10.1016/j.combustflame.2016.01.017.

[24] Yamazaki T, Matsuoka T, Nakamura Y. Near-extinction behavior of smoldering combustion under highly vacuumed environment. Proceedings of the Combustion Institute 2019;37:4083–90. doi:10.1016/j.proci.2018.06.200.

[25] Hadden RM, Rein G, Belcher CM. Study of the competing chemical reactions in the initiation and spread of smouldering combustion in peat. Proceedings of the Combustion Institute 2013;34:2547–53. doi:10.1016/j.proci.2012.05.060.

[26] Huang X, Rein G. Interactions of Earth's atmospheric oxygen and fuel moisture in smouldering wildfires. Science of the Total Environment 2016;572:1440–6. doi:10.1016/j.scitotenv.2016.02.201.

[27] Tuomisaari M, Baroudi D, Latva R. Extinguishing smouldering fires in silos: BRANDFORSK project 745-961. VTT Publications 1998:2–74.

[28] Yermán L, Wall H, Torero JL. Experimental investigation on the destruction rates of organic waste with high moisture content by means of self-sustained smoldering combustion. Proceedings of the Combustion Institute 2017;36:4419–26. doi:10.1016/j.proci.2016.07.052.

[29] Pironi P, Switzer C, Gerhard JI, Rein G, Torero JL. Self-sustaining smoldering combustion for NAPL remediation: laboratory evaluation of process sensitivity to key parameters. Environmental Science & Technology 2011;45:2980–6. doi:10.1021/es102969z.